

See discussions, stats, and author profiles for this publication at: <https://www.researchgate.net/publication/231673223>

Spread Coating of OPA on Mica: From Multilayers to Self-Assembled Monolayers

ARTICLE *in* LANGMUIR · NOVEMBER 2001

Impact Factor: 4.46 · DOI: 10.1021/la010909a

CITATIONS

41

READS

18

4 AUTHORS, INCLUDING:



Bernardo R A Neves

Federal University of Minas Gerais

82 PUBLICATIONS 1,179 CITATIONS

SEE PROFILE



Phillip E. Russell

Appalachian State University

90 PUBLICATIONS 813 CITATIONS

SEE PROFILE

Spread Coating of OPA on Mica: From Multilayers to Self-Assembled Monolayers

B. R. A. Neves,^{*,†,‡} M. E. Salmon,[§] P. E. Russell,[§] and E. B. Troughton, Jr.^{||}

Departamento de Física, UFMG, Avenida Antônio Carlos, 6627,
CEP 30123-970 Belo Horizonte, Brazil, Laboratório de Nanoscopia, CETEC,
Avenida José Cândido da Silveira, 2000, CEP 30170-000 Belo Horizonte, Brazil,
Analytical Instrumentation Facility, North Carolina State University, Box 7531,
Raleigh, North Carolina 27695, and Thomas Lord Research Center, Lord Corporation,
110 Lord Drive, Box 8012, Cary, North Carolina 27512

Received June 18, 2001. In Final Form: September 25, 2001

The process of self-assembled monolayer (SAM) formation by the spread coating of an octadecylphosphonic acid (OPA) solution onto a mica surface is investigated by atomic force microscopy. When concentrated solutions are employed, a novel mechanism of SAM formation is found: OPA multilayers, mostly bilayers, are initially deposited on the mica surface. As time passes, these large multilayers break apart and evolve into disorganized monolayers. Following a rapid evolution, such monolayers are found to transform into well-ordered OPA self-assembled monolayers.

Introduction

Self-assembled monolayers (SAMs) of different organic compounds deposited on a large variety of substrates constitute a well-established research field in the area of ultrathin films. Numerous promising industrial applications have helped to further enlarge the scientific interest in these SAM systems.^{1,2} Various types of alkanethiols deposited on flat gold surfaces represent the most traditional and studied SAM ensembles.^{3–5} In addition, several other classes of materials that also form SAMs have been proposed and carefully studied, with phosphonic acids deposited on mica being a typical example.^{6–8} Consistent with the great variety of SAM systems, there are also a significant number of SAM formation/deposition methods, such as immersion-coating, spread-coating, and vapor-phase processes. Of these methods, immersion coating is currently the most popular and widely studied. In contrast, the mechanism of the spread-coating technique as a means of SAM deposition has scarcely been investigated with modern surface science techniques such as atomic force microscopy (AFM).^{8,9} However, spread coating has significant industrial importance and might be, in several cases, the preferred method of deposition

for painting, adhesive, and soft lithography applications, where a monolayer precursor is spread-coated onto the substrate.

It is important to note that SAMs prepared by spread coating can often present the same properties as SAMs deposited by immersion coating for a given compound–substrate system.^{7–9} In other words, after the monolayer is formed, it is not possible to determine the deposition method employed by analyzing the structural properties of the SAMs formed.^{7,9} The process of SAM formation using immersion coating has been described by a sequential process of nucleation, growth, and coalescence of densely packed two-dimensional (2D) islands, finally covering the entire substrate surface or a large fraction thereof.^{7,10–13} Of particular importance to the present work, the studies of Schwartz and collaborators^{6,10,12,13} and Richards⁷ have shown that octadecylphosphonic acid (OPA) forms SAMs on mica via immersion coating following the above-described process. After investigating dilute OPA solutions, they proposed that initial 2D islands attached to mica nucleated through the adsorption of individual OPA molecules from solution.^{7,12}

In this work, the formation process of OPA self-assembled monolayers deposited on mica employing the spread-coating method is investigated using atomic force microscopy. Particular attention is paid to the SAM formation process where concentrated OPA solutions are employed. In contrast to the immersion-coating process, the spread coating of OPA from concentrated solution initially deposits OPA on mica as double- and multilayers that then transform into well-organized self-assembled monolayers.

Experimental Details

Octadecylphosphonic acid, $\text{CH}_3(\text{CH}_2)_{17}\text{PO}_3\text{H}_2$, when fully extended in the trans zigzag conformation is a linear-shaped

* Author to whom correspondence should be addressed.

† UFMG.

‡ CETEC.

§ North Carolina State University.

|| Lord Corporation.

(1) Laibinis, P. E.; Hickman, J. J.; Wrighton, M. S.; Whitesides, G. M. *Science* **1989**, *245*, 845.

(2) Ulman A. *An Introduction to Ultrathin Films*; Academic Press: New York, 1991.

(3) Troughton, E. B.; Bain, C. D.; Whitesides, G. M.; Nuzzo, R. G.; Allara, D. L.; Porter, M. D. *Langmuir* **1988**, *4*, 365.

(4) Dubois, L. H.; Nuzzo, R. G. *Annu. Rev. Phys. Chem.* **1992**, *43*, 437.

(5) Delamarche, E. B.; Kang, H.; Gerber, Ch. *Langmuir* **1994**, *10*, 4103 and references therein.

(6) Woodward, J. T.; Ulman, A.; Schwartz, D. K. *Langmuir* **1996**, *12*, 3626.

(7) Richards, J. F. MSc Thesis, North Carolina State University, Raleigh, NC, 1997.

(8) Neves, B. R. A.; Salmon, M. E.; Russell, P. E.; Troughton, E. B., Jr. *Langmuir* **2000**, *16*, 2409.

(9) Larsen, N. B.; Biebeck, H.; Delamarche, E.; Michel, B. *J. Am. Chem. Soc.* **1997**, *119*, 3017.

(10) Schwartz, D. K.; Steinberg, S.; Israelachvili, J.; Zasadzinski, J. A. N. *Phys. Rev. Lett.* **1992**, *69*, 3354.

(11) Poirier, G. E.; Pylant, E. D. *Science* **1996**, *272*, 1145.

(12) Doudevski, I.; Hayes, W. A.; Schwartz, D. K. *Phys. Rev. Lett.* **1998**, *81*, 4927.

(13) Woodward, J. T.; Doudevski, I.; Sikes, H. D.; Schwartz, D. K. *J. Phys. Chem. B* **1997**, *101*, 7535.

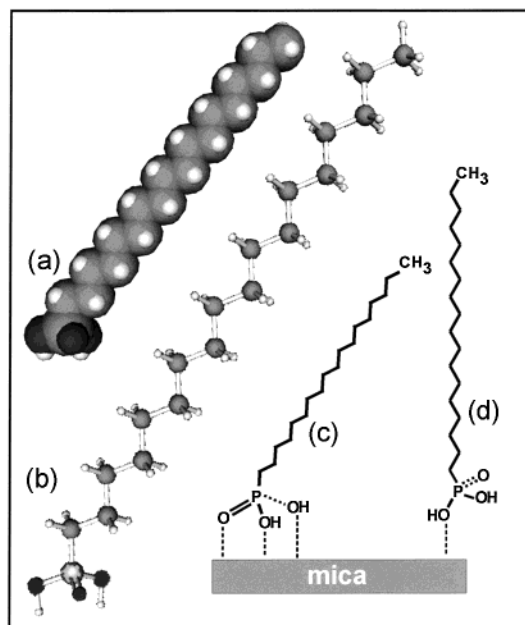


Figure 1. (a, b) Three-dimensional representations of the octadecylphosphonic acid (OPA) molecule. (c, d) Schematic drawings of the OPA molecule indicate the cases where its headgroup has triple and single bindings to the mica substrate, respectively.

lipid molecule with a length of ~ 2.5 nm.^{6,7} Figure 1a and b shows two different three-dimensional (3D) representations of the OPA molecule.¹⁴ Figure 1b represents a stereographic view of the molecule, identifying each individual atom. The smallest spheres in light gray represent H atoms, and the medium-sized spheres in dark gray at the molecule body are C atoms. The phosphonic acid attachment group (bottom of Figure 1b), is represented by the large gray sphere corresponding to the P atom and the black spheres corresponding to O atoms. Figure 1a shows almost the same representation, but with atoms occupying their appropriate volumes in space. The phosphonic acid group has three oxygen atoms that could interact with the mica surface. The exact mode by which phosphonic acid groups are attached to the mica surface could conceivably affect the conformation of the whole SAM. For example, when all three oxygen atoms of the phosphonic acid group are attached to the mica surface, the alkyl chains of the SAM must be tilted from the surface normal because of tetrahedral bonding angles around P and geometric considerations (assuming that the alkyl chain remains in the fully extended trans zigzag configuration). This conformation is represented in Figure 1a–c, showing an OPA molecule with both OH groups and the O group bound to the mica surface.¹⁴ For the case where just one OH group is bound to the mica surface, another configuration is also possible, as shown in Figure 1d.¹⁴ In this representation, the OPA molecule has its fully extended alkyl chain parallel to the surface normal.

Typically, OPA solutions have been made using either tetrahydrofuran (THF) or ethanol as the solvent, with THF being preferentially employed because the solubility of OPA is much higher in THF than in ethanol.^{6–8,12,13} Therefore, in the present work, OPA solutions ranging in concentration from 0.001 wt % (0.024 mM, ethanol solution) up to 5 wt % (133 mM, THF solution) were prepared using both solvents. The spread-coating technique employed to prepare the samples studied in this work is very simple and reproducible: A droplet (~ 10 μ L) of OPA solution is laid on a freshly cleaved mica surface, spreading over it. After a specific coating time (CT), ultrapure (99.99%) nitrogen is used to blow dry the solution from the treated mica substrate, stopping

the OPA deposition process.^{8,15} The coating time is the time interval between the instant an OPA droplet is put into contact with the mica surface and the instant it is blown from the mica substrate by a stream of nitrogen.¹⁵ In this work, the CT varied from 0.5 s to 2 min.

All samples were investigated by AFM (Digital Instruments MultiMode SPM) operating in intermittent contact (tapping) mode or in contact mode. Tapping mode was preferred to contact mode for most images because of the smaller lateral forces exerted by the scanning AFM tip on the sample surface in tapping mode. Contact mode was employed only when molecular-resolution imaging of the deposited films was required. Several (5–10) images were acquired for each sample in different regions to assess homogeneity along the sample surface. For very short coating times (CT ≤ 5 s), a slight variation of sample morphology was occasionally found. For longer coating times, the sample morphology was found to be homogeneous throughout the investigated areas.

Results and Discussion

After analysis of all samples, the results can be divided into two categories according to properties of the OPA solution employed: samples prepared with “dilute solutions” and samples prepared with “concentrated solutions”. The expression dilute solution represents the case where OPA molecules are considered to be well dissolved in the solution and considerably far apart. Therefore, the molecules might be expected to behave in solution and adsorb onto the mica surface as individual solvated entities. This is the case for OPA–THF solutions for concentrations up to 1 wt % (27 mM) and for warm (40 °C) OPA–ethanol solutions up to 0.001 wt % (0.024 mM). In contrast, for OPA–THF solutions at 5 wt % concentration (133 mM) and for OPA–ethanol solutions at concentrations greater than 0.01 wt % (0.24 mM), the results can be grouped into the concentrated solutions category. This category corresponds to the case where OPA molecules might not behave as individually solvated entities in solution, but instead, they might be associated as complex OPA aggregates in solution. In this paper, results obtained using dilute solutions are briefly discussed first in a comparison of spread-coating and immersion processes. Then, the results of similar experiments using concentrated solutions are presented and discussed in detail.

The formation of SAMs by the spread-coating process from dilute solution is very fast and seems to be analogous to the process observed for immersion-coating experiments.^{7,12} However, because of the quickness of the observed process, where SAM formation occurs in less than a few seconds (typically, less than 2 s) and also because of the simplicity of the experimental setup, it was very difficult to carefully investigate the initial phases of SAM formation. Nevertheless, upon investigating samples where the only varying parameter was the coating time, with a CT step of 0.5 s, experimental evidence of normal stages of SAM deposition was observed: nucleation, growth, and coalescence of 2D islands, resulting in the formation of typical partial-coverage OPA SAMs on the mica surface.⁸ Although the time scale is different for spread-coated samples, the results seem to be qualitatively analogous to those obtained with immersion-coated samples.^{7,12} Therefore, after these preliminary studies and because of their experimental obstacles, the formation of SAMs by the spread-coating method employing dilute solutions, which seems to present dynamics similar to those of SAMs formed by immersion coating, was not further investigated in the present work. On the other

(14) The calculation and creation of the three-dimensional molecular models of OPA shown in Figure 1a and b is a courtesy of the WebMolecules company, which can be found at www.webmolecules.com. The representations shown in Figure 1c and d were created using ChemDraw software.

(15) Neves, B. R. A.; Salmon, M. E.; Russell, P. E.; Troughton, E. B., Jr. *Microsc. Microanal.* **1999**, *5*, 413.

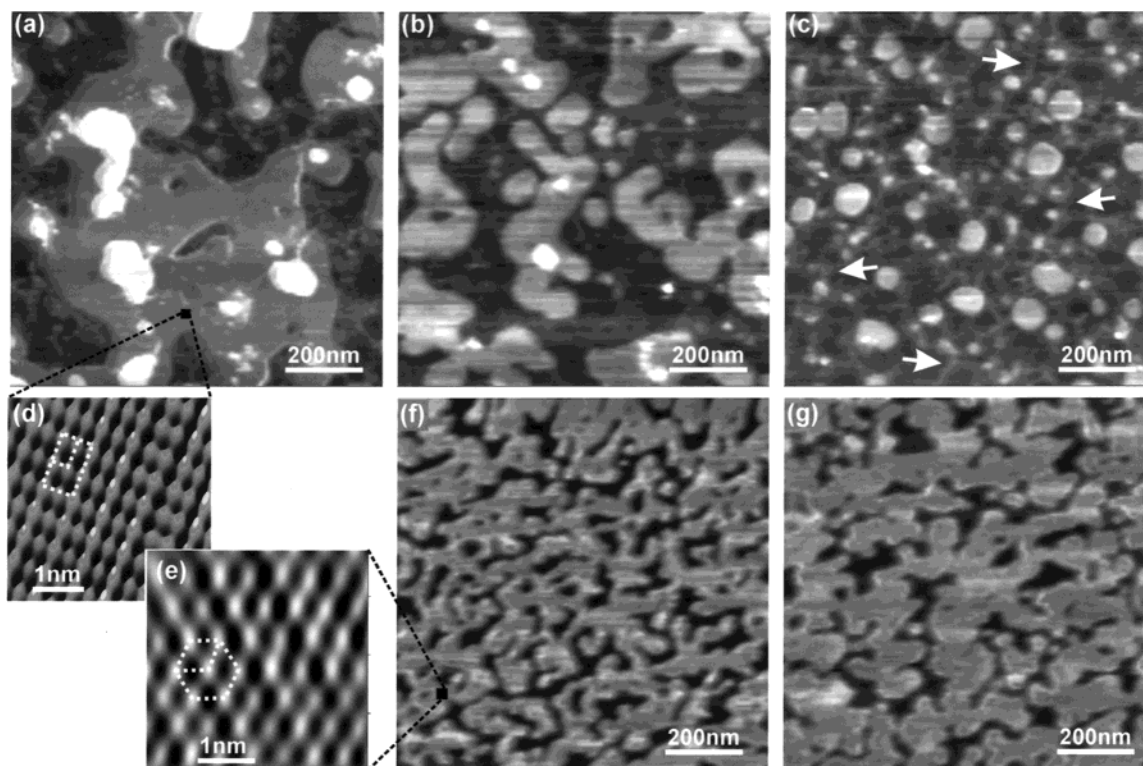


Figure 2. Atomic force microscopy (AFM) images of a series of samples prepared by spread coating using a 0.1 wt % OPA–ethanol solution. The only varying parameter in images a–c, f, and g is the coating time, which is 2, 4, 6, 10, and 25 s, respectively. These five images are $1\ \mu\text{m} \times 1\ \mu\text{m}$ in the lateral dimensions, as indicated by their scale bars. The vertical range is 15 nm for images a–c and 3 nm for images f and g. Panels d and e show high-resolution AFM images of the samples shown in a and f, respectively. A scale bar on the bottom left indicates the lateral dimensions, and the OPA molecule packing is highlighted by dotted lines on each image.

hand, samples that were prepared using concentrated solutions ($[\text{OPA}] > 0.001$ in ethanol or 5 wt % in THF) presented systematically different and unconventional results regarding the mechanism of SAM formation. Consequently, these samples were carefully investigated and constitute the object of interest for the remainder of this paper.

Figure 2 shows representative images for a series of samples prepared with a 0.1 wt % OPA–ethanol (2.4 mM) solution. The only varying parameter in Figure 2a–c, f, and g is the coating time, which was 2, 4, 6, 10, and 25 s, respectively. Figure 2d and e shows molecular-resolution images of the OPA layers in samples of Figure 2a and f, respectively. Figure 2a shows that, at very short coating times, the mica surface is covered with large 5-nm-thick OPA layers and not with small monolayer islands, as observed for SAMs formed from dilute solutions or immersion-coated samples. The dark regions in Figure 2a indicate the mica surface, gray regions indicate the first 5-nm-thick OPA layers, and white regions indicate other 5-nm-thick OPA layers on top of the first layers. Considering the geometry and length of an OPA molecule (2.5 nm), it is reasonable to suppose that a 5-nm-thick layer is an OPA double layer. Furthermore, considering the nature of OPA, it is also fair to suppose that OPA molecules are arranged in such double layers to form a conventional lipid bilayer where the hydrophobic tails face each other.¹⁶ This sample morphology was observed in a previous work and can be considered as the initial stage of OPA deposition on mica during the process of spread coating from ethanol solution at short CT.¹⁵ In Figure 2b, with CT = 4 s, it is easy to verify that large 5-nm-thick

OPA bilayers have broken into smaller layers and that there are fewer and smaller layers on top of the first OPA layers. No sign of monolayer formation can yet be observed. In Figure 2c, for CT = 6 s, 5-nm-thick layers are even smaller, and the first evidence of monolayer formation can be observed (arrows in Figure 2c indicate some of these regions). Figure 2f (CT = 10 s) shows the evolution of the previous morphology. Although the lateral range is the same as in preceding Figure 2a–c ($1\ \mu\text{m} \times 1\ \mu\text{m}$), the vertical range is different (3 nm in Figure 2f and g and 15 nm in Figure 2a–c). Therefore, the gray-scale contrast is different in these images, which explains why the sample morphology appears to be completely distinct in Figure 2c and f. In fact, if Figure 2c were printed with a vertical range of 3 nm, it would be possible to verify that the morphologies of the samples in images 2c and 2f are actually quite similar. Apart from the 5-nm-thick layers in Figure 2c, the characteristic monolayer pattern observed in Figure 2f is already forming in Figure 2c (some regions are indicated by arrows in Figure 2c). It is important to stress that no 5-nm-thick OPA bilayers are observed in the sample represented in Figure 2f. Also, it is interesting to note that the thickness of OPA SAMs is found to be ~ 1.7 nm, in agreement with previous works.^{6–8,12,13} This value of 1.7 nm is consistent with a model wherein the OPA molecules are tilted by $\sim 45^\circ$ with respect to the mica surface normal.^{6,7} Finally, in Figure 2g (CT = 25 s), the final morphology of OPA SAMs deposited on mica by spread coating is achieved.^{7,8,16} Although the surface coverage is virtually the same as for the sample in Figure 2f ($\sim 70\%$), the size of the OPA monolayers is larger in Figure 2g than in Figure 2f. In other words, the area/perimeter ratio for the monolayers increases from Figure 2f to Figure 2g.

(16) Israelachvili, J. *Intermolecular & Surface Forces*; Academic Press: New York, 1992.

Before continuing, it is useful to make some comments regarding the reproducibility of the results shown in Figure 2 as a function of coating time. Several experiments carried out using the same solution concentration showed slight deviations of the morphology with coating time. This means that, for CT = 6 s (Figure 2c), for example, the sample morphology in a few cases resembled the morphology shown in Figure 2b and, in other cases, resembled the morphology shown in Figure 2f. However, the trend of the overall morphology evolution was always reproduced, i.e., large 5-nm-thick OPA bilayers were followed by smaller bilayers; then, monolayer film formation started; and eventually, the whole substrate was overlaid by partial-coverage OPA SAMs. Similarly, the same observation holds for OPA solutions with different concentrations: although the same trend of morphology evolution as a function of CT was observed for all samples, the extent of morphological evolution at a given value of CT might be fairly different. Furthermore, a trend was observed in which the more dilute a solution was, the faster its morphological evolution.

A second important issue in this study concerns molecular order in the OPA layers. Therefore, high-resolution images of OPA layers on all samples were acquired by contact-mode AFM. A crystal-like molecular ordering was found for both 5-nm-thick OPA bilayers and SAMs. However, the molecular packing was different for each OPA layer type, as shown in Figure 2d and e. It is worth noting that no molecular order was found during the initial stages of monolayer formation, i.e., no crystal-like packing was observed in the regions indicated by arrows in Figure 2c. Figure 2e shows the conventional hexagonal packing of OPA molecules forming SAMs on mica.^{7,8} This figure is a high-resolution image of the sample represented in Figure 2f, but the same molecular packing is observed for the sample represented in Figure 2g and for any other SAM samples studied in this work. Thus, it is reasonable to conclude that this image represents the typical molecular packing for OPA SAMs on mica. Figure 2d shows the oblique (rectangular) packing of OPA molecules found in the 5-nm-thick OPA bilayer of the sample represented in Figure 2a. Again, this morphology is observed for every OPA bilayer sample investigated in this work. However, unlike the hexagonal packing of OPA SAMs, which is completely stable, the molecular packing morphology of OPA bilayers changes with the applied load of the scanning AFM tip. The situation pictured in Figure 2c represents the case where the lowest AFM tip load was applied to the bilayer (~5 nN). When the tip load was increased up to ~100 nN, the packing morphology changed, increasing the lattice spacing (first in one direction and then in both directions), and molecular superstructures could also be observed. A detailed analysis of the effect of the AFM tip load on the packing morphology is outside the scope of this paper and will be published elsewhere. For the present work, it is important only to observe that OPA bilayers do show a crystal-like structure but that this bilayer structure seems to be significantly weaker than the structure observed for the OPA SAMs.

To understand the above results, a few topics must be discussed. The first is the origin of 5-nm-thick OPA bilayers. Considering that they are observed only when concentrated solutions and very short coating times are employed, a reasonable hypothesis is to suppose that these bilayers already exist in the solution. Another hypothesis is that the formation of bilayers occurs during the blow-drying process, perhaps from crystallization or some sort of Langmuir–Blodgett deposition process. The rapid evaporation of the solvent would lead to a decrease in the

solution temperature and to supersaturation of the OPA drop on top of the mica surface. The effect of blowing the drop off the mica substrate is somewhat similar to the immersion and withdrawal process that occurs during the classical Langmuir–Blodgett deposition experiment, with the exception of the applied pressure from the sliding barrier. However, both of these mechanisms could, hypothetically, induce the formation of OPA bilayers.

The results of a few experiments carried out with the purpose of testing the two theories shed some light on the origin of the OPA bilayers. Initial hints came from light-scattering experiments on all OPA solutions that produced OPA bilayers on the mica surface. These experiments indicated the presence of large (~1 μm) aggregates in concentrated OPA solutions.¹⁷ These aggregates, which could be micelles, bilayers, and other aggregates, were not observed in dilute solutions, which also did not produce OPA bilayers.¹⁷ Although the critical micelle concentrations (CMCs) of OPA in ethanol and THF are unknown, these light-scattering results are consistent with values of ~0.2 and ~100 mM for the CMCs of OPA in ethanol and THF, respectively. Another experiment also indicated that bilayers are probably formed in solution: A 0.1 wt % OPA–ethanol solution was allowed to evaporate very slowly. After 72 h, the ethanol had completely evaporated, and a few OPA aggregates remained on the mica. These aggregates were imaged by AFM and found to be formed by 5-nm-thick OPA bilayers. Finally, well-organized OPA bilayers were also observed after spread coating, regardless of the CT, on different substrates, such as GaAs, Si, and glass.¹⁷ Therefore, there are several experimental indications that OPA bilayers attached to mica might result from the adsorption of bilayer aggregates originally present in the concentrated solutions.

After the above discussion, it is possible to picture the very initial stage of this spread-coating process: A droplet of OPA solution, containing a large number of OPA bilayer aggregates, is dripped onto the mica surface. As these bilayer aggregates contact the surface, they interact with the mica, break apart, and form layers or multilayers attached by weak interactions to the mica surface. If the micelle aggregate is assumed to have a “structure” where phosphonic acid groups are solvated by THF or ethanol and the hydrocarbon tail groups form the interior of the aggregate, then the phosphonic acid group is expected to make initial contact with the surface. After the droplet of OPA solution is removed using a stream of nitrogen, the initial structure observed by AFM is confirmed to be a multilayer structure. This structure, although stable to air, can be readily removed by rinsing with THF or ethanol, suggesting that the interaction between OPA multilayers and mica is very weak.

The next steps in the process can be better discussed with the help of Figures 1 and 3. Assuming that these 5-nm-thick layers have the same structure as typical lipid bilayers, then they can be represented by the schematic drawing in Figure 3a.¹⁶ Figure 3a represents a situation analogous to that of the image in Figure 2a, i.e., a large OPA bilayer on top of the mica surface but without a strong interaction with it. This instance would correspond to the case pictured in Figure 1d, where only one OH group is bound to the mica surface per OPA molecule. As time passes (CT increases), interactions between the phosphonic acid headgroups of OPA and the mica surface apparently develop further. As a result, the second and third bindings of the remaining OH and O headgroups start to occur, forcing the OPA molecule to acquire the

(17) Miranda, P. L.; Neves, B. R. A. Unpublished results.

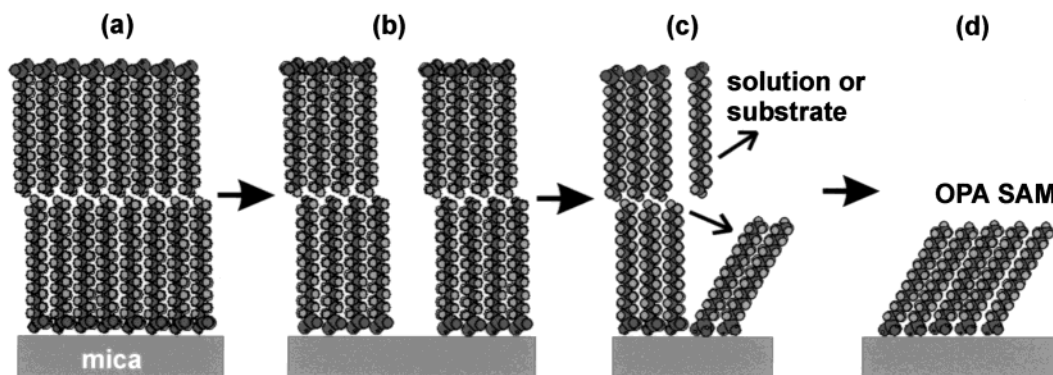


Figure 3. Schematic drawing showing the time evolution of OPA SAM formation when spread coating of concentrated solutions is employed.

configuration shown in Figure 1c. It is worth noting that a configuration consisting of an OPA–mica double-binding (not shown in Figure 1) could also be conceived as an intermediate state between the single- and triple-binding states, as suggested by the work of Reven et al. with phosphonic acids and oxide surfaces.¹⁸ As a consequence of such double- and/or triple-bindings, the alkyl chain axes are stressed laterally as they tilt, causing a bilayer to break into smaller bilayers, as pictured in Figure 2b, which corresponds to the situations shown in Figure 2b and c. With increasing CT, molecules at the boundaries of the top layer of an OPA bilayer might well desorb into solution. From this point, there are two possibilities: either a molecule dissolves back into the solution droplet, or it moves toward the substrate, with its headgroup trying to achieve the most stable configuration (Figure 1c). As a consequence of this top-layer rearrangement, the average bilayer area decreases even further, and initial formation of monolayers can be observed. This situation, pictured in Figure 3c, corresponds to the experimental result shown in Figure 2c. However, these initial monolayers do not yet present any crystal-like ordering. With further increases in the coating time, disorganized OPA molecules forming a monolayer have enough time to rearrange themselves, acquiring the most stable configuration for an OPA layer on mica: a well-ordered self-assembled monolayer. This is illustrated in Figure 3d, which is equivalent to the experimental results depicted in Figure 2e and f. Finally, for long CT, the SAMs try to decrease their interfacial free energy, which is the energy related to the covered/uncovered boundaries in the OPA–mica system, probably causing the average area/perimeter ratio of an OPA monolayer to increase. Actually, a detailed analysis of this last process would be very complicated because of the presence of water on the mica surface, which has also been shown to influence several properties of different SAMs.^{19–22}

The process discussed above represents a novel mechanism of OPA SAM formation. Instead of nucleation of small 2D islands from the adsorption of individual OPA molecules, as observed in immersion-coating processes, the present mechanism relies on the interaction between OPA headgroups and mica to transform well-organized bilayers into monolayers with distinct molecular organ-

izations. A similar process of transformation of dodecyl sulfate (SDS) hemimicellar aggregates into SAMs at Au(111) surfaces has recently been reported.²³ The proposed mechanism of SAM formation from SDS aggregates is similar to the process described in this work, which might indicate that several other organic molecule–substrate systems also undergo such a process of SAM formation.²³ The role of the OPA headgroup–substrate interaction is evident in experiments with substrates where this interaction is very small, as in oxidized GaAs and Si surfaces, where OPA bilayers are very stable and no transformation into SAMs has been observed.¹⁷

Two final interesting points to discuss are the final surface coverage and the speed of SAM formation. The final coverage is typically ~70% for OPA deposited by spread coating under the experimental conditions of this work.^{8,21} It is interesting to note that several surface properties, such as the wetting contact angle, present the same values for this coverage as for 100% covered samples.¹³ Thus, spread coating could be a useful and fast method for producing partial-coverage SAM surfaces with properties similar to those of fully covered specimens. Deposition of OPA monolayers by the spread-coating process is several orders of magnitude faster than deposition by the immersion process.^{6–8,12,13,15} One major experimental difference between the immersion process and the spread-coating process is the existence of a triple interface (the air–mica, OPA solution–mica, and OPA solution–air interfaces) for the spread-coating process. Perhaps, the existence of this triple interface is relevant to the differences observed between the spread-coating and immersion-coating processes. In addition to this triple-interface effect, the role of adsorbed water in SAM formation must not be neglected, as suggested by several works.^{19–22} A detailed discussion and modeling of these effects on the speed of OPA SAM formation is currently in progress and will be published elsewhere.

Conclusions

In conclusion, the process of OPA SAM formation by a spread-coating method using concentrated solutions has been carefully investigated. Using an interrupted-growth process, where the coating time was varied for several series of samples and solutions, several intermediate stages of the mechanism of SAM formation were observed using AFM. Initially, OPA multilayers (mostly bilayers) are deposited onto the mica surface. As the time of adsorption (CT) passes, the interaction of OPA headgroups

(18) Gao, W.; Dickinson, L.; Grozinger, C.; Morin, F. G.; Reven, L. *Langmuir* **1996**, *12*, 6429.

(19) Eastman, T.; Zhu, D. M. *Langmuir* **1996**, *12*, 2859.

(20) Beaglehole, D.; Christesson, H. K. *J. Phys. Chem.* **1992**, *96*, 3395.

(21) Neves, B. R. A.; Leonard, D. N.; Salmon, M. E.; Troughton, E. B., Jr.; Russell, P. E. *Nanotechnology* **1999**, *10*, 399.

(22) Sauer, B. B.; McLean, R. S.; Thomas, R. R. *Langmuir* **1998**, *14*, 3045.

(23) Burgess, I.; Jeffrey, C. A.; Cai, X.; Szymanski, G.; Galus, Z.; Lipkowsky, J. *Langmuir* **1999**, *15*, 2607.

with mica causes the bilayers to break into smaller layers, and then, monolayer formation begins. Initially, OPA molecules on these monolayers do not present any crystal-like ordering. Then, as time passes, they rearrange themselves, forming well-ordered self-assembled monolayers, which partially cover the mica substrate.

Acknowledgment. One of the authors (B.R.A.N.) acknowledges financial support to the Laboratorio de Nanoscopia, CETEC, from FAPEMIG (Fundação de Amparo à Pesquisa de Minas Gerais).

LA010909A